Antibiotic Discovery: from mechanistic studies to target ID
Kotsogianni, A.I.

Citation
Kotsogianni, A. I. (2023, June 20). *Antibiotic Discovery: from mechanistic studies to target ID*. Retrieved from https://hdl.handle.net/1887/3620917

Chapter 5

Chemical proteomics reveals antibiotic targets of oxadiazolones in MRSA

Abstract | Phenotypic screening is a powerful approach to identify novel antibiotics against methicillin-resistant *Staphylococcus aureus* (MRSA) infections, but elucidation of the targets responsible for antimicrobial activity is often challenging in the case of compounds with a polypharmacological mode of action. This chapter shows that activity-based protein profiling maps the target interaction landscape of a series of 1,3,4-oxadiazole-3-ones, identified in a phenotypic screen as having high antibacterial potency against multidrug resistant *S. aureus*. In situ competitive and comparative chemical proteomics with a tailor-made activity-based probe, in combination with transposon and resistance studies, revealed several cysteine and serine hydrolases as relevant targets. Our data showcase oxadiazolones as a novel antibacterial chemotype with a polypharmacological mode of action, in which FabH, FphC and AdhE play a central role.
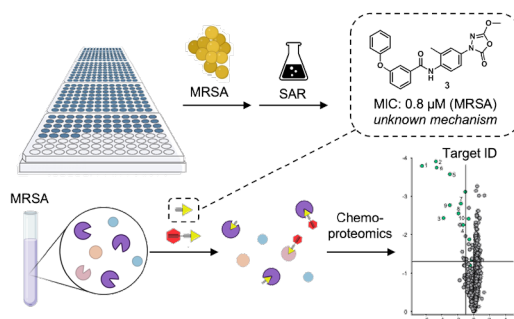
1. Introduction

The emergence of multidrug resistant bacteria combined with a dearth of new antibiotic drug approvals may become one of the biggest healthcare problems of the 21st century.[1–3] Recent data indicate that in 2019 drug resistant staphylococcal infections, due predominantly to MRSA, were associated with a staggering 750,000 deaths worldwide.[4] New antibiotics with unprecedented modes of action (MoAs) are urgently required to counteract antimicrobial drug resistance. To this end, phenotypic screening has been proven a promising approach to mine small molecule libraries and repurpose previously rejected scaffolds.[5–7] A challenging aspect of phenotypic drug discovery is, however, elucidating the primary targets responsible for the antimicrobial activity observed. In **Chapter 4**, an anti-Gram-negative hit from a bacterial growth inhibition screen was investigated. Target identification studies included genomic sequencing after selected resistant evolution experiments, and led to the development of LEI-800, as a new antibacterial chemotype acting via DNA gyrase inhibition. Recently, chemical proteomics has emerged as a powerful chemical biology technique to map target interaction landscapes of experimental drugs,[8–10] including compounds with antibacterial activity.[11,12] Inspired by these established and emerging concepts, this chapter describes a combined approach wherein phenotypic screening and chemical proteomics were applied to discover new MRSA antibiotics and their protein target landscape.

2. Results and discussion

A compound set consisting of 352 small molecules, curated from an in-house collection from the Molecular Physiology Group at the Leiden Institute of Chemistry (LIC), was first screened at 100 μM for antibacterial activity against MRSA USA300 (**Figure 1a**). This revealed 20 compounds that prevented bacterial growth (**Appendix**, **Table II.1**). Subsequently, the minimum inhibitory concentration (MIC), which is the lowest concentration at which bacterial growth is completely inhibited, was determined for each of the 20 hits. Benzyl (4-(5-methoxy-2-oxo-1,3,4-oxadiazol-3(2H)-yl)-2-methylphenyl)-carbamate **1** was the most potent antibacterial compound with a MIC of 6.25 μM (2.2 μg/mL). Compound **1** contains an oxadiazolone moiety. Oxadiazolones have been shown
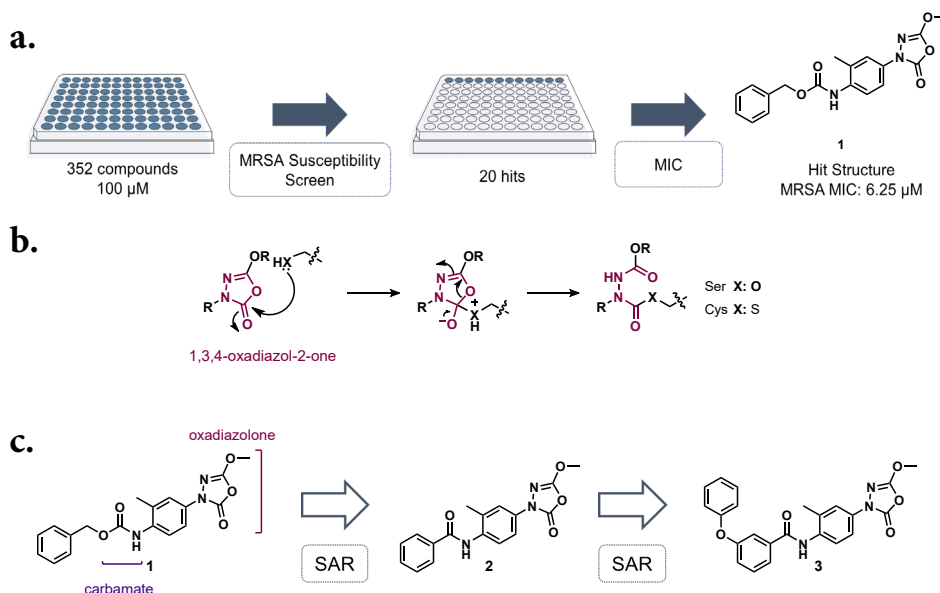
Figure 1 | Screening and hit optimization a) A single dose 352-compound library was screened against MRSA. The 20 hits were compared in an MIC assay, resulting in the most potent hit **1**. **b)** Proposed reaction mechanism of 1,3,4-oxadiazole-2-one derivatives towards reactive serine and cysteines. **c)** Structure activity relationship (SAR) investigations. Optimization of the hit structure **1** followed a disjunction approach. Modifications of the substitution pattern yielded optimized structure **3**.

to covalently react with catalytically active serine and cysteine residues in enzymes (**Figure 1b**),[13,14] and can have antibacterial activity against Mycobacteria.[15]

To determine the structure activity relationship (SAR) and optimize the potency of **1**, a series of 61 derivatives were obtained and tested for antimicrobial activity against MRSA USA300 and *S. aureus* ATCC 29213 strains (**Table S1-S6**). The oxadiazolone group and the 2-methylphenyl moiety were both found to be crucial for activity. The benzylcarbamate could be changed into a phenylamide without losing activity. This led to the identification of **2** as a simplified scaffold with comparable antibacterial activity. Subsequent systematic modification of **2** (**Figure 1c**) resulted in the discovery of *N*-(4-(5-methoxy-2-oxo-1,3,4-oxadiazol-3(2*H*)-yl)-2-methylphenyl)-3-phenoxy-benzamide **3** as our lead compound with a 16-fold improvement in potency in both MRSA USA300 (MIC = 0.8 µM, 0.3 µg/mL) and the *S. aureus* ATCC 29213 strain (MIC = 1.6 µM) compared to hit **1**.

Extended screening of **3** against other clinically relevant pathogens revealed the specific anti-staphylococcal activity of the oxadiazolones (**Table 1**). Compound **3** was found to

Table 1. Minimum inhibitory concentration (MIC) Compound **3** and clinically relevant antibiotics against a panel of bacteria. Extended data shown in **Table S7.**

Species		Strain	MIC (μM)			
			3	**MER**	**VAN**	**DAP**
Staphylococcus aureus	**MSSA**	ATCC 29213	1.6	≤0.1	0.7	1.2
	MRSA	USA300	0.8	1.1	1.4	1.2
		NY-155	0.8	9.1	0.7	1.2
		MRSA131	1.6	2.3	0.7	1.2
		COL	1.6	293	1.4	2.4
	VISA	SA MER	1.6	0.3	2.8	4.9
		LIM3	0.8	≤2.3	2.8	2.4
		NRS126	3.1	293	2.8	2.4
	VRSA	BR-VRSA	1.6	>293	88	1.2
		VRSA-1	3.1	293	88	1.2
		VRSA-2	0.8	293	88	≤0.6
Enterococcus faecium			>50	≤0.1	0.7	1.2
Gram-negative			>50	≤0.1 – 2.3	>88	>80

MER : meropenem, VAN : vancomycin, DAP : daptomycin, MSSA: methicillin-susceptible *S. aureus*, VISA: vancomycin-intermediate *S. aureus*, VRSA: vancomycin-resistant *S. aureus*.

be highly active against a variety of *S. aureu*s strains, including vancomycin resistant strains and clinical isolates. Of note, **3** was generally found to be more potent against antibiotic resistant strains compared to wild type (WT) *S. aureus*. Compound **3** was also found to be able to time-dependently kill 99% of bacteria over the course of 24 hours, starting with a 10^6 CFU/mL inoculum (**Figure 2a**). Furthermore, **3** was non-hemolytic (**Figure S1a**) and exhibited relatively low cytotoxicity (**Table S8**: selectivity ratio HEK293T/MRSA USA300 = 10.5, HepG2/MRSA300 = 20.3).

Next, we set out to generate strains resistant to **3** to investigate both the rate and mechanism of resistance development. MRSA USA300 was serially passaged daily in the presence of sub-MIC concentrations of compound, yielding resistant mutants after 4 weeks (**Figure 2b**). In comparison, resistance development for the control compound daptomycin, a clinically-used lipopeptide antibiotic, was found to be slower and did not exceed 8x MIC. This is commonly observed in cell membrane targeting antibiotics.[16,17]
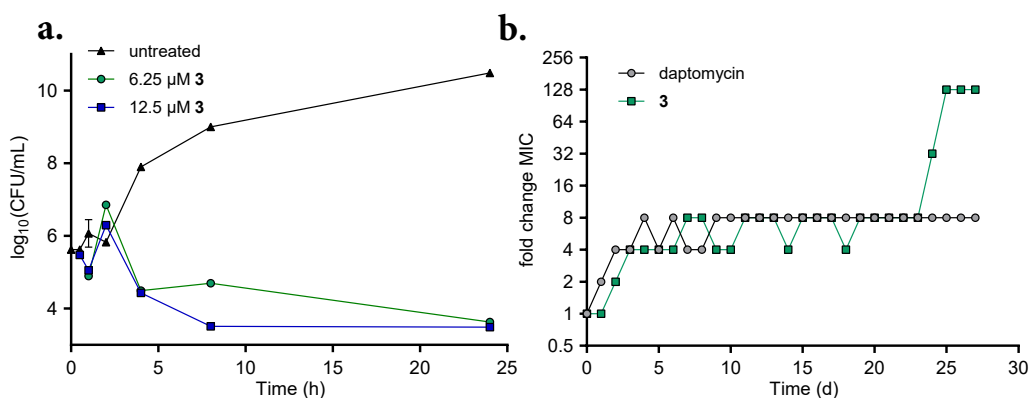
Figure 2 | *In vitro* antibacterial efficacy a) Time-dependent killing of MRSA USA300 by compound **3**. **b)** Resistance development of MRSA USA300 against **3** and daptomycin during daily passaging with 0.25x MIC concentrations. Biological replicate in **Figure S1b.**

Of note, after four days the resistance towards **3** stabilized for several weeks before progressing to significantly higher values. This may indicate that multiple mutations are required to induce high resistance, possibly suggesting a polypharmacological MoA.[18–20] Mutant strains exhibiting resistance to **3** did not show cross-resistance with commonly administered antibiotics (**Table S9**). Together with the high activity of **3** against multidrug resistant *S. aureus* strains, these observations pointed to a unique MoA.

Having established that the oxadiazolones are potent antibiotics against various pathogenic *S. aureus* strains, we set out to identify interaction partners using activity-based protein profiling (ABPP). The oxadiazolone moiety covalently reacts with catalytically active amino acids in enzymes, therefore we hypothesized that a strategically positioned alkyne ligation handle on the scaffold of **3** could be used to introduce a fluorescent or affinity tag (e.g., biotin) to visualize small molecule–protein interactions in living systems (**Figure 3a**).

To this end, the meta-phenoxy group of **3** was substituted with an alkyne, resulting in activity-based probe **4** (**Figure 3b**). The antibacterial activity of **4** was confirmed in MRSA (MIC = 3.1 μM). The probe was subsequently used in an *in situ* competitive ABPP workflow (**Figure 3a**).[21]

Briefly, MRSA USA300 was cultured until exponential phase (OD_{600} = 0.7) and treated with competitor **3** or DMSO, followed by labeling with probe **4**. Bacteria were lysed and
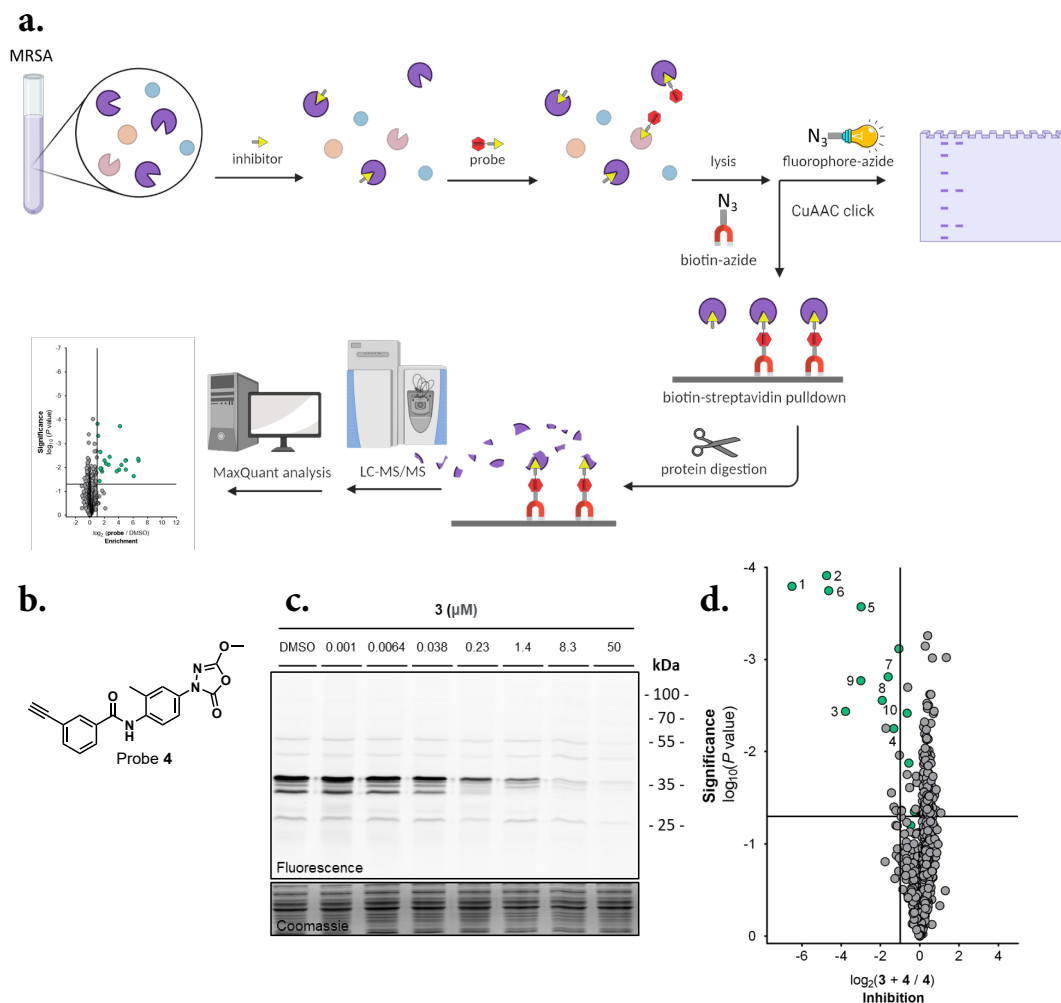
Figure 3 | a) *In situ* competitive ABPP workflow on MRSA using either SDS-PAGE or MS read-out. **b)** Activity-based probe **4**, based on the scaffold of **3**. **c)** Gel-based competitive ABPP of a concentration range of compound **3** versus 1 μM of the probe **4**. **d)** Mass spectrometry data inhibition plot comparing labelled proteome of samples preincubated with inhibitor **3** (10 μM) followed by probe **4**-labeling (3 μM) to solely probe-labelled samples. The vertical and horizontal threshold lines represent a $\log_2$ change of −1 and a $\log_{10}(P$ value) of -1.3 (two-sided two-sample t-test, n=3 independent experiments per group), respectively. Green dots indicate proteins which are probe targets, as defined in **Appendix**, **Table II.2**. *Chemical Proteomic experiments were conducted by A. T. Bakker from the group of Molecular Physiology (LIC).*

the probe-labelled proteins were conjugated to a reporter tag (fluorophore-azide or biotin-azide) via copper-catalyzed azide–alkyne cycloaddition (CuAAC, "click") chemistry.[22,23] When coupled to a fluorescent Cy5 reporter group, ABPP enables visualization of probe-labelled proteins by sodium dodecyl sulfate polyacrylamide gel electrophoresis (SDS-PAGE) and in-gel fluorescence scanning. This resulted in clear labeling of several proteins by **4**, of which most were dose-dependently outcompeted by **3** (**Figure 3c**).

To identify the probe-labelled proteins, we coupled the probe **4**-labelled proteins to a biotin reporter group, which allows affinity enrichment and identification of probe-labelled proteins by mass spectrometry (MS)-based proteomics.[24] Around 30 proteins were found to be significantly enriched ($P < 0.05$, > 2-fold enrichment) by probe treatment (**Figure S3**). Pretreatment with **3** significantly inhibited ($P < 0.05$, > 2-fold inhibition) the labeling of 10 proteins by probe **4** (**Figure 3d**, **Table 2**), suggesting that these proteins are interaction partners of oxadiazolone **3**. The Fph proteins (B, C, E, H) were recently discovered and annotated in MRSA as fluorophosphonate binding hydrolases.[25] FphB was found to be a fatty acid metabolizing virulence factor, while FphE activity has been used to phenotypically characterize MRSA through imaging.[26] Target protein HZ1 is reported to have hydrolase activity, but its biological function has not been extensively studied. IB7 is a putative acetyl-CoA *C*-acetyltransferase with thiolase

Table 2. List of probe targets significantly outcompeted by 3.

	Uniprot ID	Protein	Description	AA	Gene	Essential	Ref.
1	Q2FDS6	FphE	Uncharacterized hydrolase	276	SAUSA300_2518	No	*25,26*
2	Q2FI93	FabH	3-oxoacyl-[acyl-carrier-protein] synthase 3	313	*fabH*	Yes	*30*
3	A0A0H2XJL0	FphH	Carboxylesterase	246	*est*	No	*25*
4	A0A0H2XHZ1	HZ1	Putative lysophospholipase	271	SAUSA300_0070	No	
5	A0A0H2XHD0	FphC	Alpha/beta hydrolase	304	SAUSA300_1194	No	*25*
6	A0A0H2XHH9	HH9	Putative lipase/esterase	347	SAUSA300_0641	No	*29*
7	A0A0H2XJG5	FphB	Uncharacterized hydrolase	322	SAUSA300_2473	No	*25*
8	A0A0H2XFI2	FI2	Uncharacterized protein	275	SAUSA300_0321	No	
9	A0A0H2XIB7	IB7	Acetyl-CoA *C*-acetyltransferase	379	*vraB*	No	*27,28*
10	A0A0H2XG10	AdhE	Aldehyde-alcohol dehydrogenase	869	*adhE*	No	*34,35*

Targets 1-10 are indicated as green dots in **Figure 3d**, AA: aminoacids.

activity,[27,28] while FI2 is an uncharacterized protein. HH9 has recently been annotated as a lipase of negatively charged fatty acids.[29] FabH is an essential enzyme that initiates bacterial fatty acid synthesis[30], and has recently been explored as a drug target.[31–33] AdhE is an aldehyde alcohol dehydrogenase, essential in facultative anaerobic organisms in anaerobic conditions.[34,35] Both FabH and AdhE are known to metabolize substrates using an active site cysteine.

To confirm the identity of the probe targets with gel-based ABPP, we screened the probe-labelled proteome of nine transposon mutants of MRSA that lack the gene encoding each of the identified target proteins of **3** (**Figure 4a,c**). The labeling of AdhE, FphB, FphH, FI2, HZ1 and FphE, but not FphC and HH9, could be attributed to specific fluorescent bands on SDS-PAGE (**Figure 4b**). The lower resolution of gel-based ABPP (overlapping bands) or insufficient sensitivity compared to MS-based ABPP may explain why FphC and HH9 were not identified on gel. Since FabH is essential for MRSA viability, no transposon mutant is available for this protein. Instead, we confirmed the identity of FabH on gel by competitive ABPP using the selective FabH inhibitor Oxa2 (**Figure S2**).

To assess which target proteins were responsible for the antibiotic effect, we hypothesized that the protein labeling profile of potent oxadiazolones (MIC ≤ 12.5 μM) would be different compared to the interaction profile of their close analogues that exerted no anti-
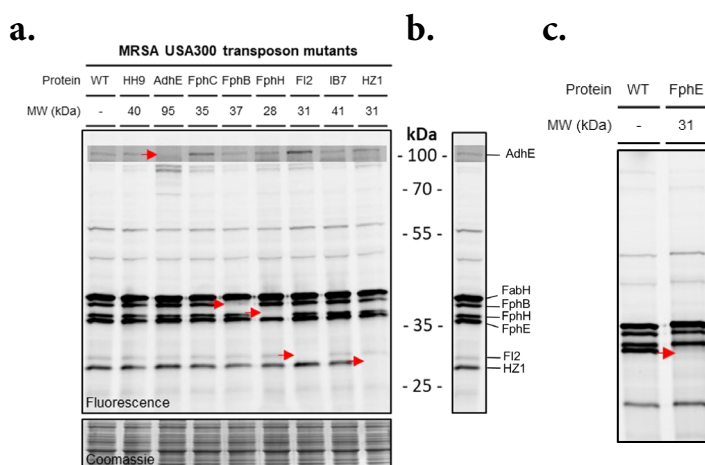
Figure 4 | On gel identification of targets a) 4 labeling of MRSA USA300 mutant strains, each with a transposon sequence inserted in genes of the identified targets of **4**. All mutants shown except FphE. **b)** WT MRSA USA300 **4** probe labeling bands annotated with corresponding proteins. **c)** labeling of the FphE transposon mutant strain. G*el-based ABPP* was *conducted by A. T. Bakker from the group of Molecular Physiology (LIC).*

MRSA activity (MIC > 50 μM). In a competitive chemical proteomics set-up, we, therefore, compared the interaction profile of three inactive derivatives (**5-7**) with three active compounds (**1-3**) (**Figure 5a**, **S5** and **Appendix II**).

Strong FphB labeling was seen in the samples pretreated with **1**, but not by the other compounds. F12, IB7, HH9 and HZ1 were not significantly labeled by the bioactive oxadiazolone **3**, but did show engagement by the inactive compounds **5, 6** or **7**. FphE and FphH were strongly labeled by all compounds at 10 μM. These observations, in combination with the viability of the transposon mutants, suggest that specific inhibition of FphB, IB7, HH9, F12, FphE, FphH or HZ1 is not responsible for the antimicrobial activity of **3**. FabH was significantly engaged, but not fully, by all compounds. Since the transposon mutant of FabH is not viable, and because Oxa2, a specific FabH inhibitor, can inhibit bacterial growth, this implies that partial inhibition of FabH activity could contribute to the bioactivity of the oxadiazolones, however, not sufficient to kill MRSA by itself. Finally, significant inhibition of FphC and AdhE labeling was only found with treatment with at least one of the bioactive compounds, but not with the inactive compounds **5-7** (**Figure 5b**).

Principal component analysis of the chemical proteomics data confirmed that inhibition of AdhE and FphC labeling was associated to a large extent with the antibacterial activity (**Table S10, Figure S4**). Thus, our chemical proteomics data reveal that multiple targets (in particular, FphC, AdhE and FabH) play a role in the observed antimicrobial activity of the oxadiazolones.

Next, we tested whether antibiotic activity of the inactive compounds **5-7** could be induced in the transposon mutants. Gratifyingly, it was observed that both **6** and **7** showed increased antimicrobial activity in both AdhE and FphC transposon mutants (**Table 3** and **S10**), but not in a FphB transposon mutant, which was taken along as a negative control. Of interest, compounds **6** and **7** did not become as active as **3**. Compound **5**, which does not inhibit AdhE and very weakly inhibits FphC labeling

Table 3. Susceptibility of MRSA USA300 target-protein transposon mutants to inactive oxadiazolones

	MIC (μM)		
	5	**6**	**7**
WT	>50	>50	>50
AdhE transposon	>50	**25**	**12.5**
FphC transposon	>50	**50**	**25**
FphB transposon	>50	>50	>50

(<20%), remained inactive in all individual transposon mutants. Interestingly, compound **7**, but not compounds **5** and **6**, regained activity against the FphE-transposon mutant (**Table S10**). No direct synergy of FabH inhibition with any single other target could be concluded as antibacterial activity of Oxa2 was not potentiated on any of the
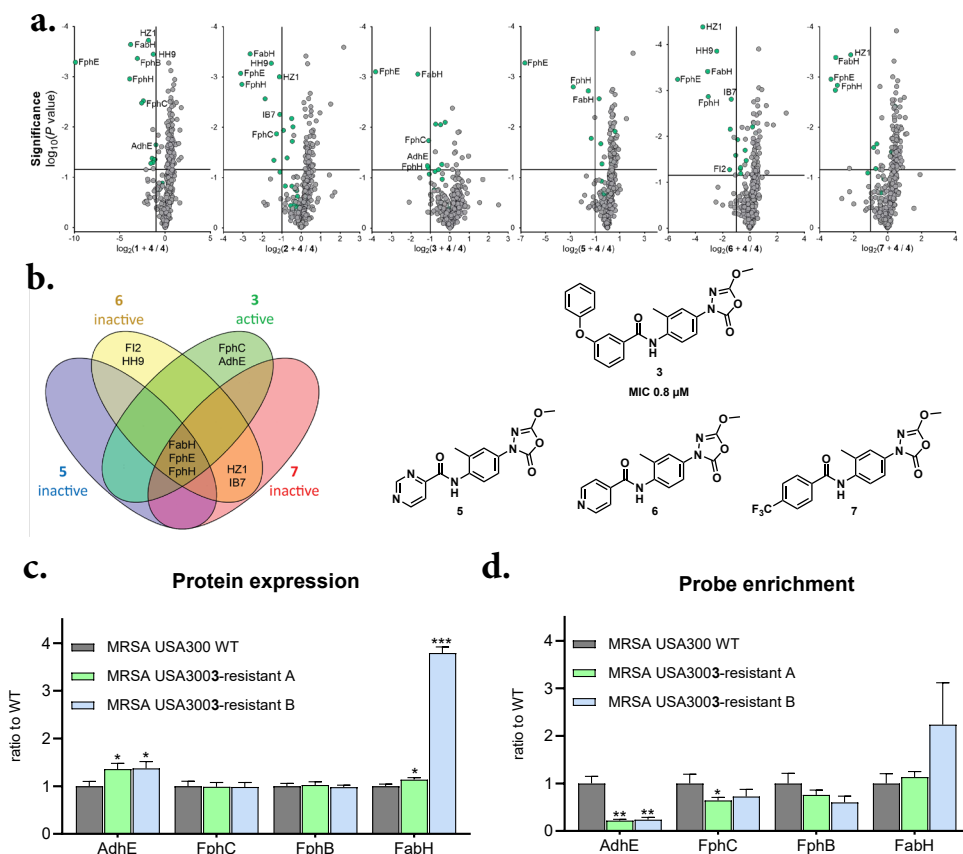

Figure 5 | a) Individual inhibition plots of active compounds **1**, **2** and **3** and inactive compounds **5**, **6** and **7**. **3** was dosed at 1 μM, while the **1**, **2**, and the inactive inhibitors were dosed at 10 μM. The vertical and horizontal threshold lines represent a $\log_2$ change of −1 and a $\log_{10}(P$ value) of -1.3 (two-sided two-sample t-test, n=3 independent experiments per group), respectively. Green dots indicate proteins which are probe targets, as defined in **Appendix**, **Table II.2** . **b)** Venn diagram showing overlap of >50% inhibited proteins between lead active compound **3** and three inactive compounds **5**, **6**, **7**. **c)** Relative general protein levels in strains resistant to **3** compared to WT. Each group was compared to WT using a two-sided two-sample t-test, n=3 independent experiments per group. Statistical significance: *** $P < 0.001$; ** $P < 0.01$; * $P < 0.05$; n.s. if $P > 0.05$. **d)** Relative protein levels enriched by **4** in strains resistant to **3** (**Figure 2b**) compared to wild-type. Each group was compared to WT using a two-sided two-sample t-test, n=3 independent experiments per group. *Chemical Proteomic experiments were conducted by A. T. Bakker from the group of Molecular Physiology (LIC).*

transposon mutants (**Table S10**). Although we cannot exclude that other proteins also play a role, we interpret these data to mean that combined engagement of FabH, FphC, AdhE and to some extent FphE is required for antimicrobial activity of the oxadiazolones.

To further test our hypothesis, we investigated whether the oxadiazolones targets were affected in two of the MRSA strains passaged to become resistant to **3** compared to WT MRSA. Using chemical (**Figure 5c** and **S6**) and global proteomics (**Figure 5d** and **S7**) it was observed that AdhE and FphE engagement of probe **4** was significantly decreased, while its protein abundance was upregulated in both resistant strains. FphC engagement was also reduced, but to a lower extent. Interestingly, FabH protein levels were significantly increased in the resistant strains, which was accompanied by cross-resistance of these strains to FabH inhibitor Oxa2 (32x increase in MIC, **Table S9**). Taken together, these data further support our hypothesis that combined inhibition of FabH, FphC, FphE and AdhE contributes to the antimicrobial activity of compound **3**.

To test if the observed proteomic differences could be related to genomic mutations, the two strains resistant to **3** were screened for mutations in the genes that encode for the 10 target proteins (**Appendix**, **Table II.5**). This revealed a single point mutation in one of the resistant strains that resulted in an amino acid change (Thr146Ile) in the FabH protein. Of note, this is also the strain in which highly upregulated FabH levels were observed.

Given the lack of other target mutations in the strains resistant to **3**, we concluded that single point mutations in target genes were not the cause of the high resistance developed to our compound, and that the observed resistance must come from other mechanisms. We hypothesized that the resistance phenotypes were unstable, and to test this the resistant strains were cultured in the absence of compound **3** for several days and then tested for susceptibility (**Figure 6**). Within a few days the MIC dropped from 128x the MIC to a consistent 8x MIC. This suggests that the observed resistance to **3** is inducible upon exposure to the compound and is lost in the absence of the compound.
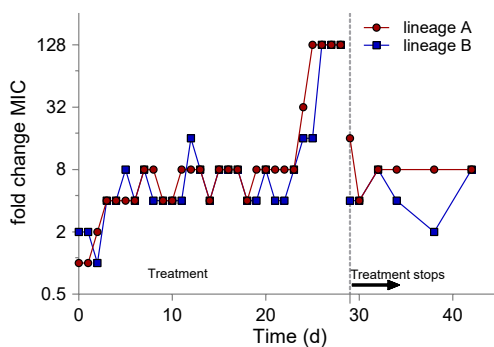
Figure 6 | Fold change MIC under selection with 3 Daily passaging of MRSA USA300 with 0.25x MIC concentrations of **3** for 28 days, followed by antibiotic free subculture for 12 days (dashed line indicates MIC of first drug free subculture).

3.   Conclusions

To summarize, a phenotypic screen of a focused library led to the identification of oxadiazolones as a new chemotype with antibiotic activity against pathogenic, multidrug resistant *S. aureus* strains and clinical isolates. A medicinal chemistry program combined with chemical proteomics led to the identification of compound **3** as the most potent antibiotic capable of interacting with multiple bacterial cysteine and serine hydrolases in a covalent manner. Three complementary lines of investigation point to FabH, FphC, AdhE and to some extent FphE as playing central roles in the antimicrobial activity of **3** and of structurally similar oxadiazolones: i) comparative chemical proteomics, ii) gain of function in transposon mutants, and iii) resistance-induced proteomic changes. FabH has previously been identified as a drug target, whereas the function of AdhE and FphC has been less well explored. Recent studies implicate AdhE as a virulence factor in *E. coli*,[36] while FphC is a predicted membrane-bound serine hydrolase of unknown function. Of note, we cannot rule out that other factors, not detected by our chemical proteomics approach, may also contribute to the antibacterial effect of **3**, such as non-covalent interactions with proteins or other classes of biomolecules. Interestingly, the resistance developed to **3** was transient, as it quickly diminished after removal of the compound, and genomic screening of target proteins in the resistant strains found only a single FabH mutation, present in one of the two **3**-selected strains. This evidence suggests that mutations in key targets are not responsible for resistance to **3**. Notably, this reversibility of resistance may be advantageous for the potential application of such compounds as antibiotics.

To conclude, our findings further highlight the value of synthetic compound libraries as a source for antibiotic drug discovery complementary to natural products. By applying comparative and competitive chemical proteomics, using a new tailor-made activity-based probe with a strategically positioned ligation tag, we successfully highlighted a multi-target MoA for the oxadiazolones and identified their probable targets in MRSA. Notably, a target-based approach alone would have not been able to uncover the oxadiazolone antibacterial mechanism, thereby showcasing the power of chemical proteomics as a valuable chemical biology technique for antibiotic drug discovery. Future experiments are directed towards understanding the biological role of these targets, the nature of the resistance, and further optimization of the compounds as viable drug candidates.

4.   Materials and Methods

Reagents and Materials Buffers and salts were of ACS reagent grade or higher and were purchased commercially, from Carl Roth GmbH (Karlsruhe, Germany) and Sigma-Aldrich (Darmstadt, Germany), biological materials and growth media were purchased from Sigma-Aldrich, Scharlab S.L. (Barcelona, Spain) and Fisher Scientific (Landsmeer, Netherlands). Antibiotics (TRC, Combi-Blocks, Sigma-Aldrich) were dissolved in ultrapure H_2O or DMSO, stock solutions were stored in -20 °C, apart from meropenem which was used fresh. All test compounds were used from 10 mM DMSO stock solutions made from freeze dried powder and stored at -20 °C.

Bacterial strains The following reagents were obtained through BEI Resources, NIAID, NIH: *Staphylococcus aureus* BR-VRSA (Strain 880, NR-49120), *S. aureus* strain MRSA131 (HM-466, as part of the Human Microbiome Project). The following *S. aureus* strains were provided by the Network on Antimicrobial Resistance in *S. aureus* (NARSA) for distribution by BEI Resources, NIAID, NIH: COL (NR-45906), NY-155 (NR-46236), USA300-0114 (NR-46070), LIM 2 (NR-45881), LIM 3 (NR-45882), NRS126 (NR-45929), NRS17 (Strain HIP06297, NR-45868), SA MER (NR-45864), VRSA-1 (Strain HIP11714, NR-46410), VRSA-2 (Strain HIP11983, NR-46411) VRSA-3a (Strain HIP13170, NR-46412), and the JE2 Transposon Mutants: NE114 (SAUSA300_0151, NR-46657), NE204 (SAUSA300_1194, NR-46747), NE104 (SAUSA300_0641, NR-46647), NE1534 (SAUSA300_0070, NR-48076), NE1227 (SAUSA300_0560, NR-47770), NE532 (SAUSA300_2473, NR-47075) NE1122 (SAUSA300_0763, NR-47665), NE1187 (SAUSA300_0321, NR-47730), NE31 (SAUSA300_2093, NR-46574). *S. aureus* USA300 (ATCC BAA1717), *S. aureus* Rosenbach (ATCC 29213) *Klebsiella pneumoniae* ATCC 29665 (NCTC 11228), *Escherichia coli* ATCC 25922, *Pseudomonas aeruginosa* ATCC 27853, *Acinetobacter baumannii* ATCC BAA747 belong to the American Type Culture Collection (ATCC). *Enterococcus faecium* E980, *E. faecium* E155, *E. faecium* E7130, were kindly provided by Dr. A.P.A. Hendrickx, National Institute for Health and Environment, Utrecht, The Netherlands.

Hemolytic activity Whole defibrinated sheep blood (10631715, Fisher Scientific) was centrifuged (400 rcf) for 15 min at 4 °C. The supernatant was discarded and the remaining blood cell suspension was mixed with phosphate buffered saline (PBS) and centrifuged (400 rcf) for 15 minutes at 4 °C. Washing cycles were repeated at least three times, until the supernatant was clear after centrifugation. The packed blood cells were diluted 25-fold in PBS with 0.002% polysorbate 80 (p80). Test compounds were serially

diluted 2-fold in U-bottom polypropylene 96-well microtiter plates in PBS with 0.002% p80 (75 µL). An equal volume (75 µL) of the blood cell suspension was added to all wells. Final concentrations of antibiotics ranged from 1.6 µM to 50 µM in triplicate. The well plates were incubated for 20 h at 37 °C with continuous shaking (500 rpm). After incubation, plates were centrifuged (800 rcf) for 5 minutes, and 25 µL of supernatant was transferred to a clear UV-star flat-bottom polystyrene 96-well plate containing 100 µL ultrapure water, per well. Absorption was measured at 415 nm with a Spark® multimode microplate reader (Tecan, Switzerland). Data were corrected for the background response of 0.5% DMSO in the presence of cells with no antibiotic and normalized using the absorbance of 0.1% Triton X-100 with blood cells, as 100% hemolytic activity.

Library screen   From glycerol stocks, USA300, as the Gram-positive representative strain, and *E. coli* W3110, as the Gram-negative representative strain, were cultured on blood agar plates (PB5039A, Thermo Scientific) by overnight (18 ± 2 h) aerobic incubation at 37 °C. A single colony was transferred to tryptic soy broth (TSB) or lysogeny broth (LB). The cultures were grown to exponential phase (OD_{600} = 0.5) at 37 °C. The bacterial suspensions were diluted 200-fold in cation adjusted Mueller-Hinton broth (CAMHB) and 99 µL were added in a library of test compounds (1 µL DMSO stock solution, per well in technical duplicates) in polypropylene 96-well microtiter plates to reach a volume of 100 µL and a final concentration of 100 µM for each test compound and a maximum of 1% DMSO. The plates were sealed with breathable membranes and incubated at 37 °C for 18 ± 2 h with constant shaking (600 rpm). Screening hits were selected from the wells where no visible bacterial growth was observed, as compared to the inoculum controls, containing 1% DMSO.

Minimum inhibitory concentration (MIC)   From glycerol stocks, bacterial strains were cultured on blood agar plates by overnight incubation at 37 °C. A single colony was transferred to TSB. In case of VRSA strains, 6 µg/mL vancomycin was supplemented to the media. The cultures were grown to exponential phase (OD_{600} = 0.5) at 37 °C. The bacterial suspensions were diluted 100-fold in CAMHB and 50 µL was added to a 2-fold serial dilution series of test compounds (50 µL per well) in polypropylene 96-well microtiter plates to reach a volume of 100 µL. The plates were sealed with breathable membranes and incubated overnight at 37 °C with constant shaking (600 rpm). For *Enterococci species* direct colony suspension was used by immediately suspending multiple colonies from fresh blood agar plates in CAMHB to an OD_{600} of 0.5 and subsequent 100-fold dilution. The MIC was determined as the lowest concentration at

which no visible bacterial growth was observed, as compared to the inoculum controls, from the median of a minimum of triplicates.

Minimum bactericidal concentration (MBC) For minimum bactericidal concentration (MBC) determination, 96-well plates were prepared likewise in biological duplicate. After incubation, 100 μL of each bacterial culture corresponding to 1, 2, 4, 8 and 16× MIC was centrifuged for 5 min (12500 rpm). The supernatant was discarded and pellets were washed once with filter-sterilized PBS, then resuspended in an equal volume of fresh buffer and samples were diluted with a 10-fold factor. 10 μL of the appropriate dilutions were inoculated on LB agar plates in technical duplicates and incubated at 37 °C for 18 h. The colonies were counted and used to calculate the CFU/mL of the original culture. The MBC was determined as the lowest concentration of the test compound that was able to produce a 99.9% decrease in viable bacterial cells.

Time-kill assay From glycerol stocks, bacterial strains were cultured on blood agar plates by overnight incubation at 37 °C. Subsequently, a single colony was cultured in TSB overnight at 37 °C. The culture was diluted 100-fold in fresh CAMHB and grown until early exponential phase (OD_{600} = 0.25) followed by 100-fold dilution in media (OD_{600}: 0.0025). The culture was split in separate culture tubes containing 2 mL. Test compounds were added to the cultures at concentration 3.1 μM and 6.2 μM (corresponding to 4 and 8× MIC) and incubated at 37 °C for a total of 24 h. At indicated time points (t: 0, 1/2, 1, 2, 4, 8 and 24 h) 100 μL of each culture was centrifuged for 5 min (12500 rpm). The supernatant was discarded and pellets were washed once with filter-sterilized PBS, then resuspended in an equal volume of fresh buffer and samples were 10-fold serially diluted until 10^5 dilution. 10 μL of the appropriate dilutions were inoculated on LB agar plates in technical duplicates and incubated at 37 °C for 18 h. The colonies were counted and used to calculate the CFU/mL remaining in the original culture by taking the dilution factors into account. Experiments were performed in biological duplicates.

Resistance induction assay From glycerol stocks, bacterial strains were cultured on blood agar plates by overnight incubation at 37 °C. A single colony was grown to exponential phase (OD_{600} = 0.5) in TSB and diluted 100-fold in fresh media. In polypropylene 96-well microtiter plates, antibiotics were added and serial diluted 2-fold by transfer and mixing from one well to the next to achieve a final volume of 50 μL per well. An equal volume of bacterial suspension was added to the wells and plates were incubated at 37 °C for 18 h. Bacterial cultures corresponding to 0.25× MIC were diluted

100-fold in fresh media and added (50 µL per well) to a newly prepared antibiotic dilution series (50 µL per well) followed by incubation at 37 °C for 18 h. This procedure was repeated for 30 days and the MIC was recorded daily. The experiment was performed in biological triplicates and for each replicate the MIC was determined from the median of a minimum of triplicates. In order to obtain spontaneous resistant colonies, 100 µL of USA300 inoculum grown to an OD_{600} of 0.5 was plated onto LB agar containing 5x the MIC of compound **3**. The plates were incubated at 37 °C and inspected for growth every 12 h for a maximum of 48 h. Single colonies were picked after 48 h and their MIC was determined as described previously. No change in MIC was observed.

Mammalian cell culture HepG2 and HEK293T cell lines (ATCC) were cultured at 37 °C and 7% CO_2 in DMEM (Sigma Aldrich, D6546) with GlutaMax, penicillin (100 µg/mL), streptomycin (100 µg/mL) and 10% Fetal Calf serum. Cells were passaged twice a week by first detaching using 0.05% trypsin in PBS, and then diluting to appropriate confluence.

Cytotoxicity assay (MTT) Compound cytotoxicity was evaluated against HepG2 and HEK293T human cell lines using standard (3-(4,5-dimethylthiazol-2-yl)−2,5-diphenyltetrazolium bromide (MTT) assay protocol[37] with slight changes. HepG2 and HEK293T cells were seeded at a density of 1.5×10^4 cells per well in a clear 96-well tissue culture treated plate in a final volume of 100 µL in Dulbecco's Modified Eagle Medium (DMEM), supplemented with Fetal Bovine Serum (1%), Glutamax and Pen/Strep. Cells were incubated for 24 h at 37 °C, 7% CO_2 to allow cells to attach to the plates. In addition to a single vehicle control, compounds (diluted from DMSO stock) were added into each well at eight concentrations ranging from 100 µM to 0.046 µM in three-fold dilutions (final DMSO concentration 0.5%). Incubation was done for 24 h at 37 °C, 7% CO_2. After the incubation, MTT was added to each well at a final concentration of 0.40 mg/mL. The plates were then incubated for 2 h at 37 °C, 7% CO_2. Medium was carefully removed via suction, and purple formazan crystals were resuspended in 100 µL DMSO. Absorbance was read at 570 nm using a Clariostar plate reader. The data was then analysed with GraphPad Prism software. CC_{50} values were calculated using non-linear fitted curve with variable slope settings, with values adjusted for background (plotted ABS_{SAMPLE} = (ABS_{SAMPLE} − $ABS_{BACKGROUND}$) / ($ABS_{VEHICLE}$ − $ABS_{BACKGROUND}$)). Technical triplicates for each condition were used, along with two biological replicates. The reported CC_{50} was obtained by averaging the calculated CC_{50} of both biological replicates.

Sample preparation ABPP Several bacterial colonies were suspended in LB medium in sterile Erlenmeyer flasks and grown in aerobic conditions at 37 °C shaking at 270 rpm. At an OD_{600} of at least 0.70, the cells were divided in 50 mL fractions and harvested by centrifugation (5000 rcf, 10 min, 4 °C), and were then washed with PBS once. For each fraction, the pellet was resuspended in 1000 μL PBS, then the samples were pooled and divided into 396 μL samples in 1.5 mL Eppendorf tubes. To each sample 1.5 μL DMSO or inhibitor (200× concentrated) was added and the samples were incubated on a thermo-shaker (600 rpm, 37 °C) for 1 h. 1.5 μL probe (200× concentrated, final concentration 3 μM) or DMSO was then added and the samples were further incubated (37 °C, 600 rpm, 30 min). Cells were pelleted by centrifugation (5000 rcf, 10 min, 4 °C) and washed with PBS once. Pellets were then resuspended in 300 μL PBS/0.2% SDS (+ Roche cOmplete™ protease inhibitor cocktail) and lysed by bead beating (3× 50 s at 6 m/s).
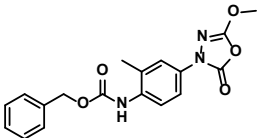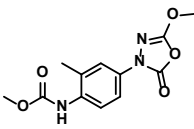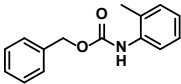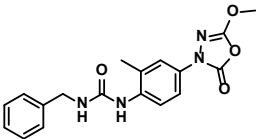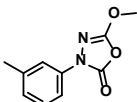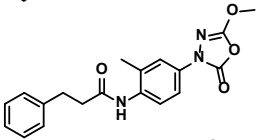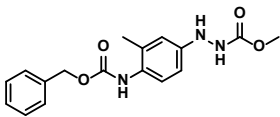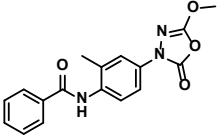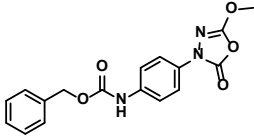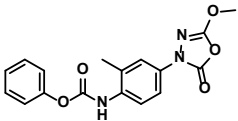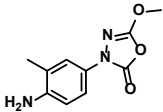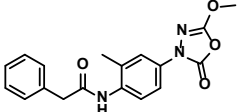
Gel-based ABPP and in-gel fluorescence analysis 18 μL of lysate was clicked with Alexa647-azide (Invitrogen, A10277) by adding 2 μL click mix (10×, 10 mM $CuSO_4$, 56.56 mM sodium ascorbate, 2 mM THPTA, 40 μM Alexa647-azide in Milli-Q) and incubating at room temperature for 1 h. The reaction was quenched by addition of 5 μL Laemmli buffer (4×, 240 mM Tris-HCl pH 6.8, 8% w/v SDS, 40% glycerol, 5% v/v β-mercapto-ethanol, 0.04% v/v bromophenol blue), followed by heating (95 °C, 5 min). The samples were resolved by SDS-PAGE (12.5% acrylamide gel, 15-wells, 10 μL per well) at 180 V for 80 min, after which the gels were imaged at Cy3 and Cy5 channels on a ChemiDoc Imaging System (Bio-Rad). Gels are checked for equal protein loading with Coomassie Brilliant Blue staining. Images were processed using ImageLab software (Bio-Rad).

Supplementary Information

Synthetic procedures and whole proteome results can be found in full in the online version of the manuscript https://doi.org/10.1021/jacs.2c10819. The following information is available in **Appendix II:** experimental section for the MS-based proteome analysis; methods and primers used for PCR amplification and sequencing.

Supplementary Tables

Table S1. SAR Table: Dissecting structure **1** for antibacterial activity.

ID	Structure	MRSA	SA	ID	Structure	MRSA	SA
		MIC (μM)				**MIC (μM)**	
1		6.25	12.5	13		50	>50
8		>50	>50	14		>50	>50
9		>50	>50	15		25	>50
10		>50	>50	2		12.5	25
11		25	>50	16		>50	>50
12		>50	>50	17		12.5	50

In this and subsequent tables: MRSA: methicillin resistant *S. aureus* USA300, SA: *S. aureus* ATCC 29213.

Table S2. SAR Table: Middle ring derivatives

ID	R	MRSA	SA	ID	R	MRSA	SA
		MIC (μM)				**MIC (μM)**	
2		12.5	25	20	Cl	25	50
18	H	>50	>50	21	NC	25	>50
19	O	25	>50				

Table S3. SAR Table: Left ring variations of compound **2**.

ID	R	MIC (µM) MRSA	MIC (µM) SA	ID	R	MIC (µM) MRSA	MIC (µM) SA
2		12.5	25	31		6.25	>50
6		>50	>50	32		6.25	12.5
22		50	>50	33		12.5	>50
23		>50	>50	34		>50	>50
24		>50	>50	35		12.5	25
5		>50	>50	36		>50	>50
25		>50	>50	37		25	>50
26		6.25	50	4		3.13	25
27		6.25	>50	38		25	>50
28		12.5	>50	3		0.8	1.6
29		6.25	25 - 50	39		25	50
30		6.25	25	40		1.6	>50
7		>50	>50				

Table S4. SAR Table: Variations of compound **3**.
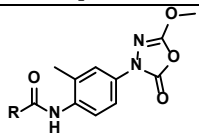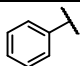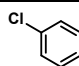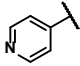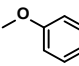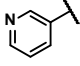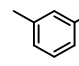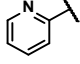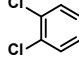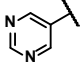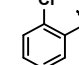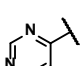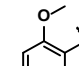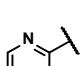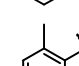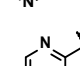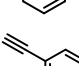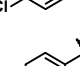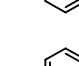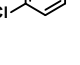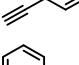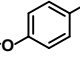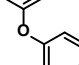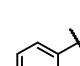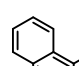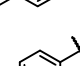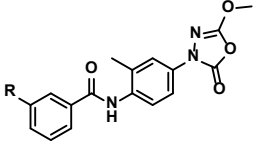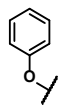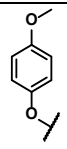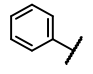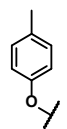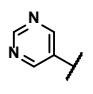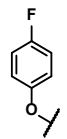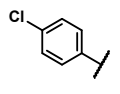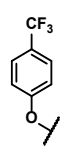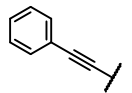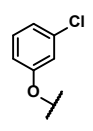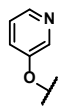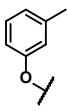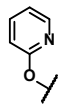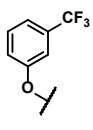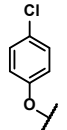
ID	R	MIC (µM)		ID	R	MIC (µM)	
		MRSA	SA			MRSA	SA
3		0.8	1.6	48		1.6	3.1
41		>12.5	>50	49		3.1	1.6
42		12.5	>50	50		1.6	3.1
43		>12.5	>50	51		3.1	>12.5
44		>12.5	>50	52		0.8 – 1.6	3.1 – 6.25
45		>12.5	>50	53		0.8	1.6 – 3.1
46		12.5	>50	54		1.6	>12.5
47		1.56	3.13				

Table S5. SAR Table: Warhead variations of compound **3.**

ID	R	MIC (μM)	
		MRSA	SA
3		0.8	1.6
55		>12.5	>12.5
56		>12.5	>12.5
57		>12.5	>12.5
58		>12.5	>12.5

Table S6. SAR Table: Oxadiazolone side chain variations of compound **3.**

ID	R	MIC (μM)	
		MRSA	SA
3		0.8	1.6
59		0.8	3.1
60		>12.5	>12.5
61		1.6	>12.5
62		3.1	>12.5

Table S7. Extended MIC Data of compounds **1-3** and common antibiotics.

MIC µM (µg/mL)							
Species	**Strain**	**1**	**2**	**3**	**meropenem**	**vancomycin**	**daptomycin**
MRSA	USA300	6.25 (2)	12.5 (4)	0.8 (0.3)	1.1 (0.5)	1.4 (2)	1.2 (2)
Staphylococcus aureus	ATCC 29213	25 (8.9)	25 (8)	1.6 (0.7)	≤0.1 (≤ 0.06)	0.7 (1)	1.2 (2)
MRSA	NY-155	3.1 (1.1)	12.5 (4)	0.8 (0.3)	9.1 (4)	0.7 (1)	1.2 (2)
MRSA	MRSA131	3.1 (1.1)	6.25 (2)	1.6 (0.7)	2.3 (1)	0.7 (1)	1.2 (2)
MRSA	COL	6.25 (2.2)	25 (8)	1.6 (0.7)	293 (128)	1.4 (2)	2.4 (4)
MRSA	NRS384	1.6 (0.6)	3.1 (1)	1.6 (0.7)	4.6 (2)	0.7 (1)	1.2 (2)
MRSA & VISA	LIM2	6.25 (2.2)	12.5 (4)	1.6 (0.7)	4.6 (2)	2.8 (4)	1.2 (2)
VISA	SA MER	12.5 (4.4)	>50 (>16)	1.6 (0.7)	0.3 (0.13)	2.8 (4)	4.9 (8)
VISA	LIM3	6.25 (2.2)	12.5 (4)	0.8 (0.3)	≤2.3 (≤1)	2.8 (4)	2.4 (4)
VISA	NRS126	25 (8.9)	50 (16)	3.1 (1.3)	293 (128)	2.8 (4)	2.4 (4)
VISA	NRS17	25 (8.9)	50 (16)	3.1 (1.3)	9.1 (4)	5.5 (8)	0.6 (1)
VRSA	BR-VRSA	12.5 (4.4)	25 (8)	1.6 (0.7)	>293 (>128)	88.3 (>128)	1.2 (2)
VRSA	VRSA-1	25 (8.9)	50 (16)	3.1 (1.3)	293 (128)	88.3 (>128)	1.2 (2)
VRSA	VRSA-2	6.25 (2.2)	25 (8)	0.8 (0.3)	293 (128)	88.3 (>128)	≤0.6 (≤1)
VRSA	VRSA-3a	12.5 (4.4)	25 (8)	1.6 (0.7)	146.3 (64)	88.3 (>128)	≤0.6 (≤1)
Pseudomonas aeruginosa	ATCC 27853	>50 (>18)	>50 (>16)	>50 (>21)	2.3 (1)	88.3 (>128)	>79 (>128)
Acinetobacter baumannii	ATCC BAA747	>50 (>18)	>50 (>16)	>50 (>21)	0.6 (0.25)	88.3 (>128)	>79 (>128)
Klebsiella pneumoniae	ATCC 29665	>50 (>18)	>50 (>16)	>50 (>21)	≤0.1 (≤ 0.06)	88.3 (>128)	>79 (>128)
Escherichia coli	ATCC 25922	>50 (>18)	>50 (>16)	>50 (>21)	≤0.1 (≤ 0.06)	88.3 (>128)	>79 (>128)
Enterococcus faecium	E155	50 (18)	>50 (>16)	50 (21)	36.6 (16)	44.2 (64)	≤0.6 (≤1)
Enterococcus faecium	E7130	50 (18)	>50 (>16)	50 (21)	>293 (>128)	≤0.7 (≤1)	9.9 (16)

MRSA, methicillin-resistant *Staphylococcus aureus*, VISA, vancomycin intermediate *S. aureus*, VRSA, vancomycin resistant *S. aureus*.

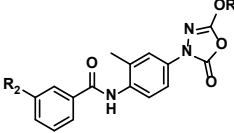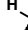**Table S8. Human cytotoxicity** Cytotoxicity of selected derivatives.
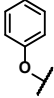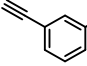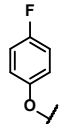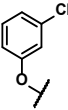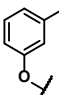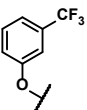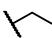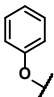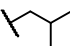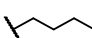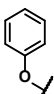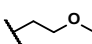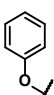
ID	R1	R2	CC50 (µM)		MIC (µM)		Selectivity ratio (HEK293T/ MRSA)	Selectivity ratio (HepG2/ MRSA)
			HEK293T	HepG2	MRSA	SA		
1			46	>50	12.5	25	3.7	>4.0
3			8.4	16.2	0.8	1.6	10.5	20.3
4			10.2	>50	3.1	25	3.3	>16.1
50			8.2	25	1.6	3.1	5.1	15.6
52			4.4	11	0.8 – 1.6	3.1 – 6.25	2.7 - 5.5	6.9 - 13.8
53			3.9	6.3	0.8	1.6 – 3.1	4.9	7.9
54			15	11	1.6	>12.5	9.4	6.9
59			9.4	7.2	0.8	3.1	11.8	9.0
60			>50	>50	>12.5	>12.5	-	-
61			16	>50	1.6	>12.5	10.0	>31.3
62			4.6	7.0	3.1	>12.5	1.5	2.3

Table S9. MIC resistant mutants: MIC of antibiotics against strains selected for resistance to **3**.

	MIC (µM)		
	USA300	**3**-resistant A	**3**-resistant B
Compound **3**	0.8	>50	>50
Probe **4**	3.1	>50	>50
Meropenem	2.3	2.3	2.3
Vancomycin	0.7	0.7	0.7
Daptomycin	1.2	1.2	1.2
Rifampicin	0.015	0.015	0.015
Novobiocin	0.13	0.13	0.13
Chloramphenicol	12.5	12.5	12.5
Ciprofloxacin	>100	>100	>100
Oxa2	0.4	12.5	12.5

Table S10. Antibacterial activity of compounds **1-3**, **5-7** against transposon mutants.

NTML strain	Locus	Transposon	MIC (µM)						
			1	**2**	**3**	**5**	**6**	**7**	Oxa2
		WT	6.25	12.5	0.8	>200	>200	>50	0.4
NE114	151	AdhE	6.25	12.5	0.8	>200	**25**	**12.5**	0.4
NE204	1194	FphC	6.25	12.5	0.8	>200	50	**25**	0.4
NE532	2473	FphB	6.25	12.5	0.8	>200	100	>50	0.4
NE104	641	HH9	6.25	12.5	0.8 / 1.6	>200	50	50	0.4
NE1534	70	HZ1	6.25	12.5	0.8	>200	100	>50	0.8
NE1227	560	IB7	6.25	25	0.4 / 0.8	>200	50	>50	0.8
NE1122	763	FphH	6.25	25	0.8	>200	100	>50	0.8
NE1187	321	FI2	6.25	25	0.8	>200	100	>50	0.4
NE1779	2518	FphE	6.25	6.25	0.8	>200	50	**12.5**	0.4

NTML: Nebraska Transposon Mutant Library.
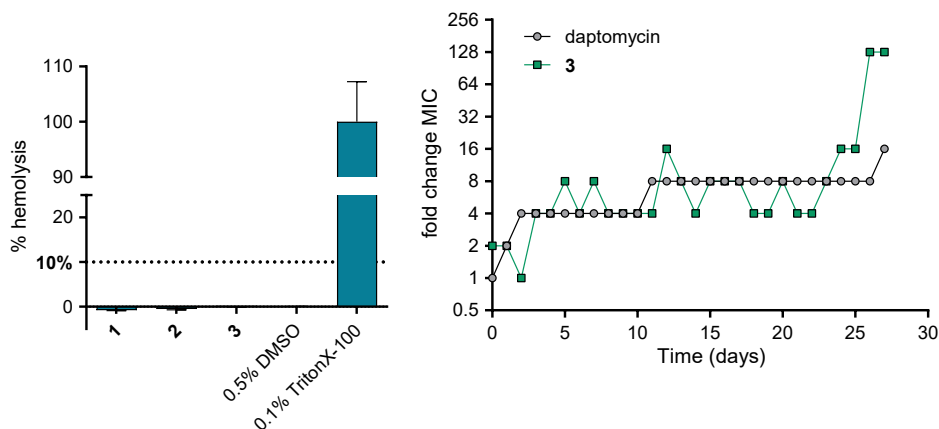
Supplementary Figures

Figure S1 | a) Normalized hemolytic activity of oxadiazolone compounds **1**-**3** at 50 µM after 20 h incubation time. **b)** Resistance development of MRSA USA300 against **3** and daptomycin during daily serial passaging with 0.25× MIC concentrations. Second biological replicate (**3**-resistant B isolated at day 28). Biological replicate 1 is shown in **Figure 2b**.
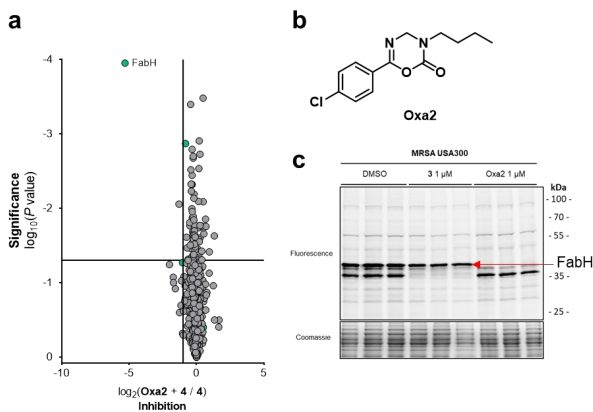
Figure S2 | Chemical proteomics data Oxa2 reveals FabH band on SDS-PAGE   a) Mass spectrometry data inhibition plot comparing labelled proteome of samples preincubated with Oxa2 (1 µM) followed by probe-labeling (3 µM) to solely probe-labelled samples. The vertical and horizontal threshold lines represent a $\log_2$ change of −1 and a $\log_{10}(P$ value) of -1.3 (two-sided two-sample t-test, n=3 independent experiments per group), respectively. **b)** Structure of Oxa2. **c)** Gel-based competitive ABPP of indicated inhibitors followed by incubation with probe **4** (3 µM).
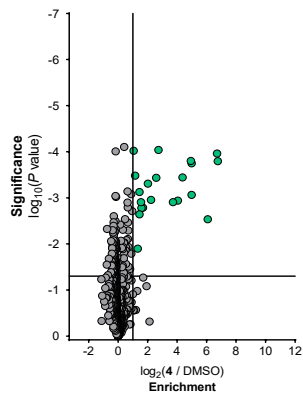
Figure S3 | a) Mass spectrometry data enrichment plot comparing labelled proteome of **3** μM **4**-treated MRSA to DMSO-treated MRSA. The vertical and horizontal threshold lines represent a $\log_2$ change of 1 and a $\log_{10}(P$ value) of -1.3 (two-sided two-sample t-test, n=3 independent experiments per group), respectively. Green dots indicate proteins which are probe targets (>2-fold enriched, $P < 0.05$). Probe targets annotated in **Appendix**, **Table II.2**.

Figure S4 | PCA analysis of the inhibition profiles of the six compounds (left). Contribution of individual protein inhibition levels to PC1 and PC2 (right). Loadings principal component 2 contributions are found tabulated in **Appendix**, **Table II.3**.

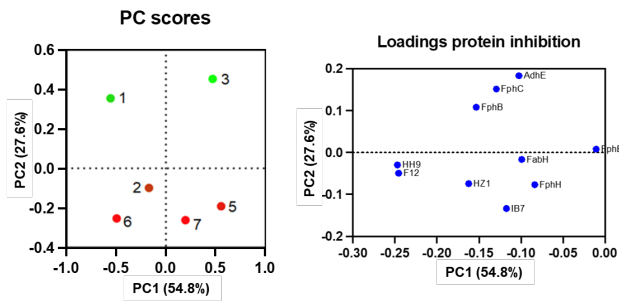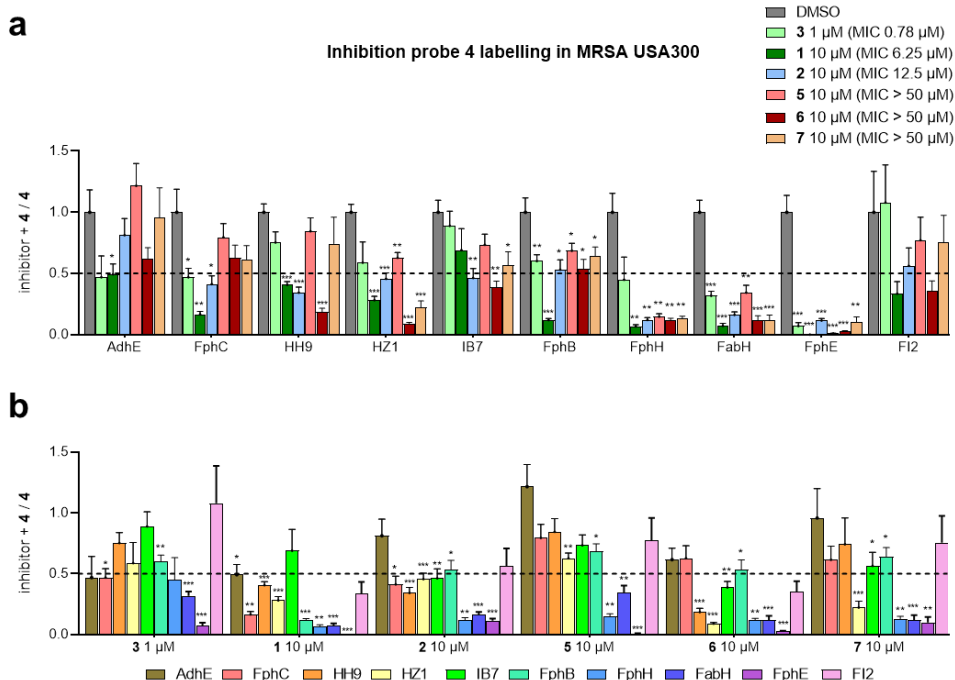**Figure S5** | Bar graphs key protein inhibition in inactive ABPP experiment. All groups consist of n=3 independent replicates. Statistical data was obtained by two-sided two-sample t-test, where every inhibitor-treated condition was tested against DMSO-treated control. Statistical significance: *** P <0.001; ** P < 0.01; * P < 0.05; n.s. if P > 0.05. **a)** Bar graph inhibition profile per protein. **b)** Bar graph inhibition profile per inhibitor.
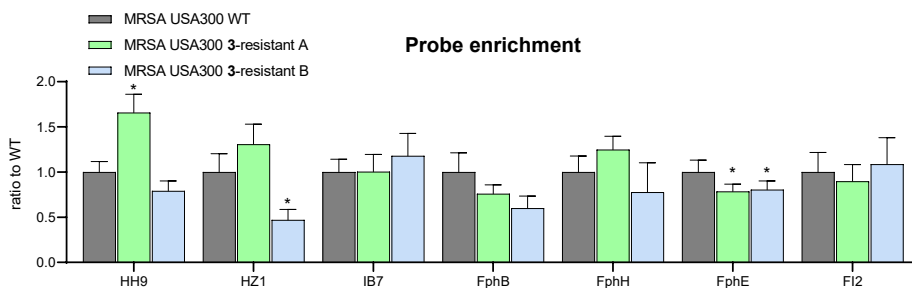
Figure S6 | Graph probe enrichment remaining targets. Each group was compared to WT using a two-sided two-sample t-test, n=3 independent experiments per group. Statistical significance: *** P <0.001; ** P < 0.01; * P < 0.05; n.s. if P > 0.05.

Figure S7 | Full graph protein expression. IB7 was not identified. Each group was compared to WT using a two-sided two-sample t-test, n=3 inde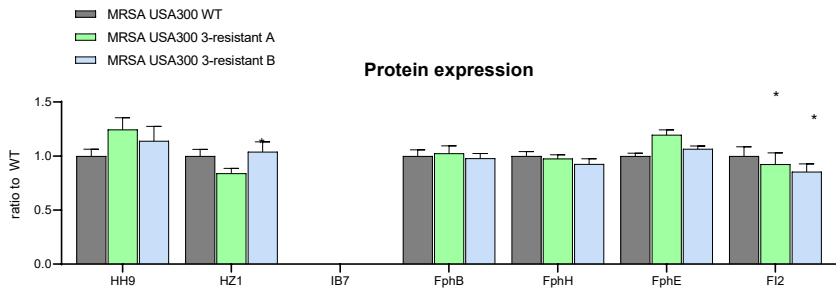pendent experiments per group. Statistical significance: *** P <0.001; ** P < 0.01; * P < 0.05; n.s. if P > 0.05.

References

1. Tacconelli, E. *et al.* Discovery, Research, And Development Of New Antibiotics: The WHO Priority List Of Antibiotic-Resistant Bacteria And Tuberculosis. *Lancet Infect. Dis.* **18**, 318–327 (2018).

2. Lewis, K. The Science Of Antibiotic Discovery. *Cell* **181**, 29–45 (2020).

3. Brown, E. D. & Wright, G. D. Antibacterial Drug Discovery In The Resistance Era. *Nature* **529**, 336–343 (2016).

4. Murray, C. J. *et al.* Global Burden Of Bacterial Antimicrobial Resistance In 2019: A Systematic Analysis. *Lancet* **399**, 629–655 (2022).

5. Urahn, S. K. *et al.* A Scientific Roadmap For Antibiotic Discovery. *Pew Charit. Trust.* 1–42 (2016).

6. Aulner, N., Danckaert, A., Ihm, J. E., Shum, D. & Shorte, S. L. Next-Generation Phenotypic Screening In Early Drug Discovery For Infectious Diseases. *Trends in Parasitology* vol. 35 559–570 at https://doi.org/10.1016/j.pt.2019.05.004 (2019).

7. Swinney, D. C. Phenotypic Vs. Target-Based Drug Discovery For First-In-Class Medicines. *Clin. Pharmacol. Ther.* **93**, 299–301 (2013).

8. Van Esbroeck, A. C. M. *et al.* Activity-Based Protein Profiling Reveals Off-Target Proteins Of The FAAH Inhibitor BIA 10-2474. *Science (80-.).* **356**, 1084–1087 (2017).

9. Klaeger, S. *et al.* The Target Landscape Of Clinical Kinase Drugs. *Science (80-.).* **358**, eaan4368-18 (2017).

10. Bar-Peled, L. *et al.* Chemical Proteomics Identifies Druggable Vulnerabilities In A Genetically Defined Cancer. *Cell* **171**, 696-709.e23 (2017).

11. Le, P. *et al.* Repurposing Human Kinase Inhibitors To Create An Antibiotic Active Against Drug-Resistant *Staphylococcus Aureus*, Persisters And Biofilms. *Nat. Chem.* **12**, 145–158 (2020).

12. Hübner, I. *et al.* Broad Spectrum Antibiotic Xanthocillin X Effectively Kills *Acinetobacter Baumannii* Via Dysregulation Of Heme Biosynthesis. *ACS Cent. Sci.* acscentsci.0c01621 (2021).

13. Nguyen, P. C. *et al.* Oxadiazolone Derivatives, New Promising Multi-Target Inhibitors Against *M. Tuberculosis*. *Bioorg. Chem.* **81**, 414–424 (2018).

14. Ben Ali, Y. *et al.* Use Of An Inhibitor To Identify Members Of The Hormone-Sensitive Lipase Family. *Biochemistry* **45**, 14183–14191 (2006).

15. Madani, A. *et al.* Dissecting The Antibacterial Activity Of Oxadiazolone-Core Derivatives Against *Mycobacterium Abscessus*. *PLoS One* **15**, 1–19 (2020).

16.   Roch, M. *et al.* Daptomycin Resistance In Clinical MRSA Strains Is Associated With A High Biological Fitness Cost. *Front. Microbiol.* **8**, 1–9 (2017).

17.   Igler, C., Rolff, J. & Regoes, R. Multi-Step Vs. Single-Step Resistance Evolution Under Different Drugs, Pharmacokinetics, And Treatment Regimens. *Elife* **10**, 1–24 (2021).

18.   Brotz-Oesterhelt, H. & Brunner, N. A. How Many Modes Of Action Should An Antibiotic Have? *Curr. Opin. Pharmacol.* **8**, 564–573 (2008).

19.   East, S. P. & Silver, L. L. Multitarget Ligands In Antibacterial Research: Progress And Opportunities. *Expert Opin. Drug Discov.* **8**, 143–156 (2013).

20.   Peters, J.-U. Polypharmacology – Foe Or Friend? *J. Med. Chem.* **56**, 8955–8971 (2013).

21.   Van Rooden, E. J. *et al.* Mapping In Vivo Target Interaction Profiles Of Covalent Inhibitors Using Chemical Proteomics With Label-Free Quantification. *Nat. Protoc.* **13**, 752–767 (2018).

22.   Kolb, H. C., Finn, M. G. & Sharpless, K. B. Click Chemistry: Diverse Chemical Function From A Few Good Reactions. *Angew. Chemie Int. Ed.* **40**, 2004–2021 (2001).

23.   Meldal, M. & Tornøe, C. W. Cu-Catalyzed Azide–Alkyne Cycloaddition. *Chem. Rev.* **108**, 2952–3015 (2008).

24.   Tyanova, S., Temu, T. & Cox, J. The MaxQuant Computational Platform For Mass Spectrometry-Based Shotgun Proteomics. *Nat. Protoc.* **11**, 2301–2319 (2016).

25.   Lentz, C. S. *et al.* Identification Of A S. Aureus Virulence Factor By Activity-Based Protein Profiling (ABPP) Article. *Nat. Chem. Biol.* **14**, 609–617 (2018).

26.   Chen, L., Keller, L. J., Cordasco, E., Bogyo, M. & Lentz, C. S. Fluorescent Triazole Urea Activity-Based Probes For The Single-Cell Phenotypic Characterization Of *Staphylococcus Aureus*. *Angew. Chemie - Int. Ed.* **58**, 5643–5647 (2019).

27.   Meriläinen, G., Poikela, V., Kursula, P. & Wierenga, R. K. The Thiolase Reaction Mechanism: The Importance Of Asn316 And His348 For Stabilizing The Enolate Intermediate Of The Claisen Condensation. *Biochemistry* **48**, 11011–11025 (2009).

28.   Diep, B. A. *et al.* Complete Genome Sequence Of USA300, An Epidemic Clone Of Community-Acquired Methicillin-Resistant *Staphylococcus Aureus. Lancet* **367**, 731–739 (2006).

29.   Kumar, N. G., Contaifer, D., Wijesinghe, D. S. & Jefferson, K. K. *Staphylococcus Aureus* Lipase 3 (SAL3) Is A Surface-Associated Lipase That Hydrolyzes Short Chain Fatty Acids. *PLoS One* **16**, 1–14 (2021).

30.   Lai, C. Y. & Cronan, J. E. β-Ketoacyl-Acyl Carrier Protein Synthase III (FabH) Is Essential For Bacterial Fatty Acid Synthesis. *J. Biol. Chem.* **278**, 51494–51503 (2003).

31.   Wang, J. *et al.* Discovery Of Platencin, A Dual FabF And FabH Inhibitor With In Vivo Antibiotic Properties. *Proc. Natl. Acad. Sci. U. S. A.* **104**, 7612–7616 (2007).

32.   Luo, Y., Yang, Y. S., Fu, J. & Zhu, H. L. Novel FabH Inhibitors: A Patent And Article Literature Review (2000 2012). *Expert Opin. Ther. Pat.* **22**, 1325–1336 (2012).

33.   Wang, J. *et al.* Discovery Of Novel Antibiotics As Covalent Inhibitors Of Fatty Acid Synthesis. *ACS Chem. Biol.* **15**, 1826–1834 (2020).

34.   Fuchs, S., Pané-Farré, J., Kohler, C., Hecker, M. & Engelmann, S. Anaerobic Gene Expression In *Staphylococcus Aureus*. *J. Bacteriol.* **189**, 4275–4289 (2007).

35.   Lo, J., Zheng, T., Hon, S., Olson, D. G. & Lynd, L. R. The Bifunctional Alcohol And Aldehyde Dehydrogenase Gene, AdhE, Is Necessary For Ethanol Production In *Clostridium Thermocellum* And *Thermoanaerobacterium Saccharolyticum*. *J. Bacteriol.* **197**, 1386–1393 (2015).

36.   Beckham, K. S. H. *et al.* The Metabolic Enzyme AdhE Controls The Virulence Of *Escherichia Coli* O157: H7. *Mol. Microbiol.* **93**, 199–211 (2014).

37.   Sigma-Aldrich. Protocol Guide: MTT Assay For Cell Viability And Proliferation. *Merck KGaA* 5–7 (2021).